IDO1 and TDO inhibitory evaluation of analogues of the marine pyrroloiminoquinone alkaloids:wakayin and tsitsikammamines

Thomas Levy[a], Laura Marchand[a], Vincent Stroobant[b], Luc Pilotte[b], Benoît Van den Eynde[b], Frédéric Rodriguez[a] and Evelyne Delfourne[a,*]

a)Université Paul Sabatier, UMR CNRS 5068, Laboratoire de Synthèse et Physicochimie de Molécules d'Intérêt Biologique, 118 Route de Narbonne, 31062 Toulouse Cédex 9, France.

b)Ludwig Cancer Research Ltd (Brussels Branch) & de Duve Institute (Tumor Immunology & Antigen Processing group), Avenue Hippocrate 74 (UCL B1.7403) B-1200 Bruxelles, Belgique.

Abstract:

Indoleamine 2,3-dioxygenase (IDO1) and tryptophane 2,3-dioxygenase (TDO) are two heme-containing enzymes which catalyze the conversion of tryptophan to N-formylkynurenine. Both enzymes are well establish therapeutic targets as important factors in the tumor immune evasion mechanism. A number of analogues of the marine pyrroloquinoline alkaloids tsitsikammamines or wakayin have been synthesized, two of them were synthesized using an original method to build the bispyrroloquinone framework. All the derivatives were evaluated in a cellular assay for their capacity to inhibit the enzymes. Six compounds have shown a significant potency on HEK 293-EBNA cell lines expressing hIDO1 or hTDO.

Keywords: marine alkaloids, pyrroloiminoquinone, bispyrroloquinone, wakayin, tsitsikammamine, IDO1 and TDO.

* Corresponding author, Tel 33 561 55 62 93 ; Fax 33 561 55 60 11
E-mail : delfourn@chimie.ups-tlse.fr

1. Introduction

In the recent period, immunotherapy has proven to be a promising method for cancer treatment. Among the enzymes involved in the mechanisms allowing tumors to resist or escape immune rejection, indoleamine-2,3-dioxygenase (IDO1) and tryptophane-2,3-dioxygenase (TDO) play an essential role.[1,2] They are two main enzymes which catalyse the rate-determining first step of the tryptophan catabolization along the Kynurenine pathway. Despite the continuous efforts to develop IDO1 and TDO inhibitors, only nine compounds have reached clinical trials[3], of which, only two target both the two enzymes. This indicates that there is still an urgent need for the discovery of new molecules with this mode of action.

Exiguanine A, a marine alkaloid isolated from the sponge *Neopetrosia exigua*, has been reported so far, as the most potent IDO1 inhibitor obtained from natural source (Ki = 41 nM).[4] In our group we are interested in a family of alkaloids, mainly found in sponges and ascidians, based on the pyrrolo[4,3,2-*de*]quinolone scaffold, and more particularly in a subgroup of this class of compounds including wakayin[5] and tsitsikammamines A and B[6], which possess a unique tetracyclic bispyrroloiminoquinone ring system.

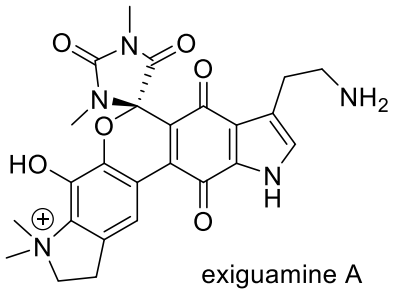

exiguamine A

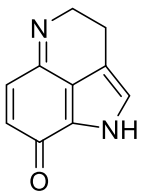

pyrrolo[4,3,2-de]quinolone

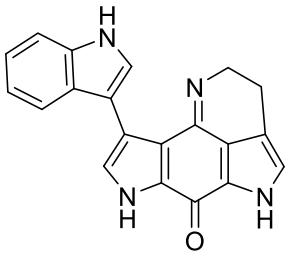

wakayin

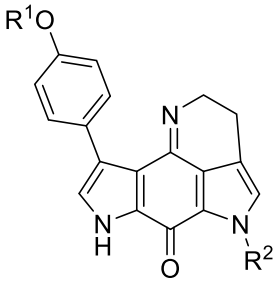

tsitsikammamine A, $R^1 = R^2 = H$
tsitsikammamine B, $R^1 = H$, $R^2 = Me$
methoxytsitsikammamine , $R^1 = Me$, $R^2 = H$

***Figure 1**: Alkaloids obtained from marine source*

As part of our research program to define new anticancer agents, we were led to study IDO1 and TDO inhibitory activities of tsitsikammamines analogues involved in the synthesis of tsitsikammamine A.[7,8] Some of the compounds described, including methoxy-tsitsikammamine have shown submicromolar potency in an enzymatic assay whereas a number of other were also active against IDO1 in a cellular assay.[9] Recently, the structurally related derivative Roxyl-WL which constitutes one of the most highly potent and selective inhibitor targeting IDO1 discovered so far (IC_{50} = 1 nM), has been described.[10]

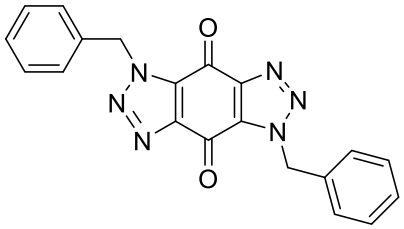

***Figure 2**: Roxyl-WL*

This context prompted us to evaluate IDO1 and TDO inhibitory potency of compounds **1**-**20** in a cellular assay, the results are reported herein.

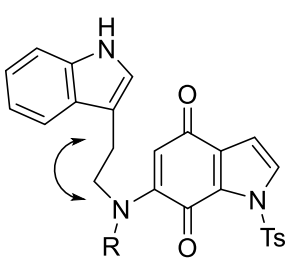

1 R = H, iso1
2 R = H, iso2

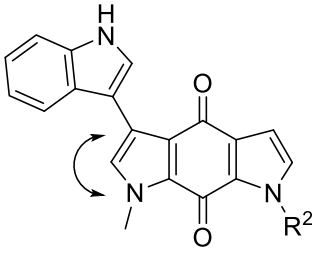

3 iso1
4 iso2

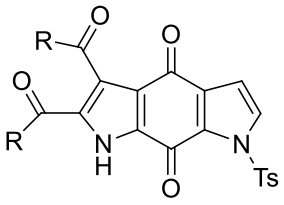

5 R = Ph
6 R = Ph(OMe)
7 R = indole

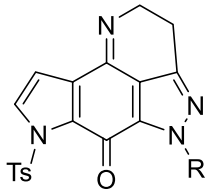

8 R = Ts
9 R = H

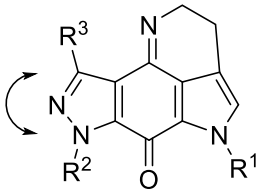

10 R^1 = Ts, R^2 = R^3 = H, iso1
11 R^1 = Ts, R^2 = R^3 = H, iso2
12 R^1 = R^2 = R^3 = H, iso2
13 R^1 = Ts, R^2 = H, R^3 = Ph, iso1
14 R^1 = Ts, R^2 = H, R^3 = Ph, iso2
15 R^1 = H, R^2 = H, R^3 = Ph, iso1
16 R^1 = Ts, R^2 = H, R^3 = Ph(OH), iso1
17 R^1 = Ts, R^2 = H, R^3 = Ph(OH), iso2
18 R^1 = H, R^2 = H, R^3 = Ph(OH), iso1
19 R^1 = Ts, R^2 = Me, R^3 = H
20 R_1 = Ts, R^2 = H, R^3 = 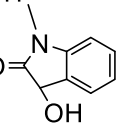 , iso1

***Figure 3**: Analogues of the marine alkaloids wakayin and tsitsikammamine*

2. Results and discussion

Chemistry

Compounds **1**-**4** were prepared by adapting the reaction sequence previously reported by Zhang *et al.*, the methoxy-naphtoquinone being replaced by N-tosylindoledione **21**.[11]

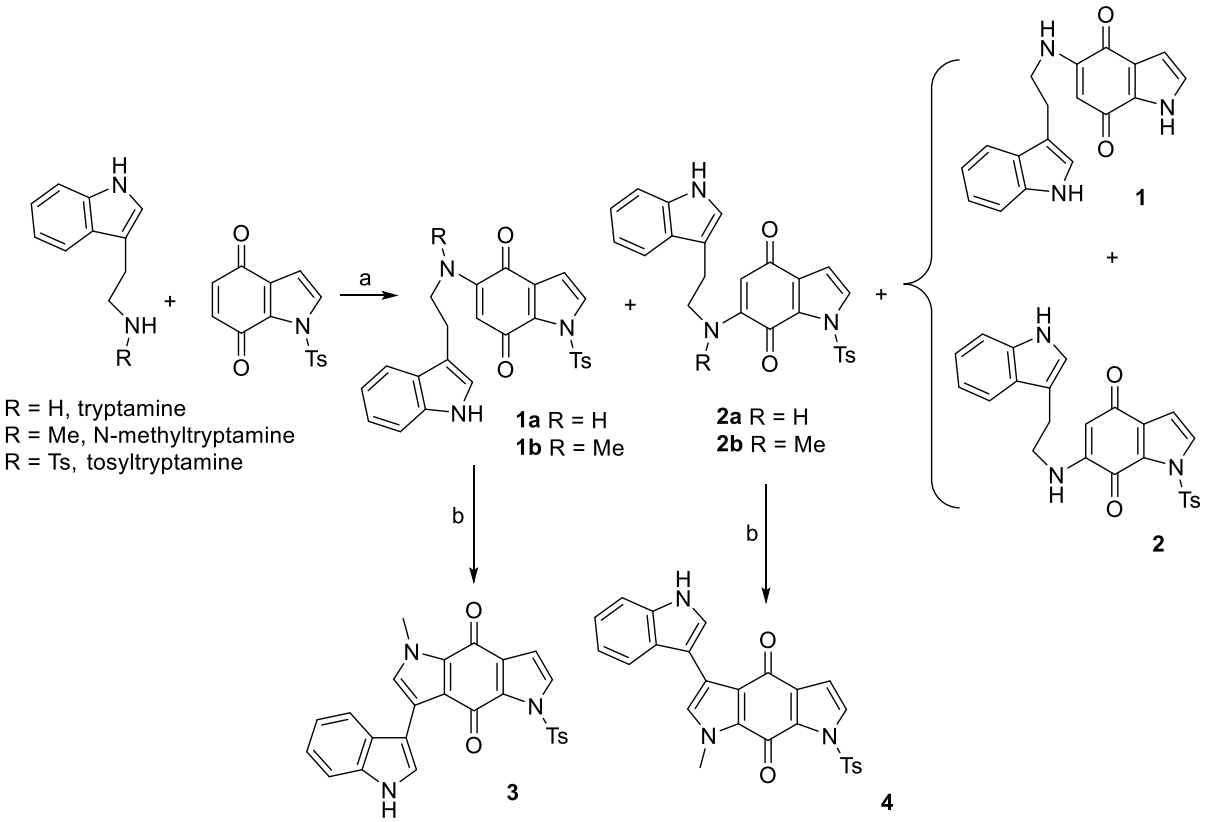

a- EtOH, RT, 2h (**1a** 8%, **2a** 11%, **1** 46%, **2** 22%; **1b** 12%, **2b** 48%). b- DDQ, CH_2Cl_2 (**3** 28%, **4** 75%).

Scheme 1**: Synthesis of analogues **1-4

In the first step, 1-tosyl-1H-indole-4,7-dione was condensed with tryptamine to give a mixture of two regioisomers **1a** and **2a** both with their corresponding detosylated analogues **1** and **2** in 8, 11, 46 and 22% yield respectively. It has to be noted that tosyltryptamine was isolated as a by-product.[12] The same reaction in which tryptamine was replaced by N-methyl tryptamine led to compounds **1b** and **2b** which were subsequently reacted with DDQ to form derivatives **3** and **4** (28 and 75% yield respectively). The structural assignment of these compounds was achieved from a previously described empirical method.[13] It has to be noted that this last synthetic sequence constitutes a new strategy to build the bispyrroloquinonic framework. Derivatives **5**-**7** were obtained by action of an indoledione on different β-ketoamines[14], whereas pyrazolic analogues **8**-**20** have been prepared on the basis of a [3+2] dipolar

cycloaddition reaction between various quinones and diazo species as previously reported by our group.[15,16]

Bioactivity assay

The synthesized derivatives were evaluated for their ability to inhibit tryptophane degradation and kynurenine production in HEK 293-EBNA cell lines expressing hIDO1 or hTDO cell lines expressing IDO1 and TDO. This global cellular assay is informative for drug development, as it evaluates a combination of the drugs' TDO/IDO inhibitory potency, their potential cytotoxicity, the inhibition of tryptophan transporters, and the effects of their metabolites. The assay was performed as previously described, the results are reported in Table1.[17]

Table 1*: Inhibition and cell viability data for wakayin and tsitsikammamine analogues*

Compounds	Viability	IDO	TDO	Viability	IDO	TDO	Viability	IDO	TDO	Viability	IDO	TDO
	25 µM	**25µM**		12.5 µM	**12.5 µM**		6.25 µM	**6.25 µM**		3.12 µM	**3.12 µM**	
	mean	mean	mean	mean	mean	mean	mean	mean	mean	mean	mean	mean
1	26	39±1.3	67±0.6	56	38±1.7	31±0.4	69	28±0.7	12±0.3	75	23±0.1	5±2.9
2	84	11±0	0±1.0	99	13±1.6	0±0.0	98	9±1.1	-3±1.3	98	2±0.7	-8±1.5
3	95	28±0.6	-8±1.7	97	26±1.1	-1±1.2	98	20±1.6	2±1.4	100	12±0.0	2±0.4
4	88	27±1.4	-3±1.3	96	21±0.2	0±0.1	96	12±0.8	3±3.1	98	8±0.4	2±1.3
5	111	61±1.6	28±4.1	102	62±0.2	55±0.0	125	58±0.2	27±0.9	99	52±0.6	15±0.7
6	100	63±0.5	-1±1.8	105	63±1.1	3±0.4	97	63±0.4	6±2.2	94	61±0.1	4±0.6
7	75	24±0.1	-9±1.7	82	25±0.1	-2±0.1	81	22±0.4	1±3.9	87	16±1.1	-1±1.5
8	67	-88±1.4	-35±5.9	85	-80±1.4	-34±1.5	88	-58±2.1	-28±2.6	87	-55±5.2	-19±0.2
9	115	-3±0.6	3±0.8	110	-4±0.8	-6±1.1	98	-3±3.1	-7±0.3	107	0±3.5	-7±1.7
10	91	6±0.9	7±2.0	97	9±0.8	13±0.5	91	9±1.6	14±1.1	92	10±0.4	12±1.0
11	93	11±1.1	15±1.1	110	15±0.9	23±0.3	106	12±0.6	19±1.9	87	10±0.1	15±0.2
12	90	-1±0.1	9±1.3	91	0±0.5	8±2.2	92	2±0.2	8±1.4	93	2±0.7	6±3.0
13	78	18±0.5	-10±4.0	79	16±0.0	2±5.4	95	12±0.9	5±1.2	91	10±0.2	5±2.8
14	96	23±0.3	21±1.4	123	22±0.4	18±4.1	126	19±0.7	13±1.7	91	14±3.4	10±1.2
15	84	5±0.1	5±0.2	94	5±1.1	6±0.7	93	4±1.2	5±0.2	93	4±2.0	3±1.5
16	63	18±5.4	12±2.4	65	11±0.8	-4±1.3	80	7±0.3	-2±0.3	87	5±0.8	-3±0.4
17	136	20±0.5	0±2.1	121	14±0.1	-10±1.1	86	6±0.6	-6±1.9	90	3±1.8	-8±1.0
18	84	3±0	1±3.4	96	2±1.8	-4±3.1	98	0±2.2	0±0.6	103	-1±0.1	-9±3.0
19	72	36±1.1	35±1.2	77	23±0.2	21±2.9	89	16±2.8	18±0.2	93	11±0.8	3±0.1
20	31	14±2.0	27±2.0	84	1±0.8	6±0.2	107	3±0.2	5±1.6	104	1±1.3	-7±1.2

IDO and TDO cell assay inhibition: Inhibitory activity (%) was estimated by measuring tryptophan degradation and kynurenine production in the supernatant of 24-h cultures performed in the presence of compound at different concentrations. Tryptophan and kynurenine were measured by HPLC. Cell viability (%) was estimated by an MTS/PMS assay in the same cultures. The indicated values are the result of two to four independent determinations.

Among the twenty compounds tested in the present study, six: **1**, **3**, **5**, **6**, **7** and **19** exhibit inhibitory activities ranging from 23 to 63% against IDO1 at 12.5 μM with only two of which **5** and **6** retain good activity when their concentration was reduced to 3.12 μM. Three of these derivatives **1**, **5** and **19** are also active against TDO at the same concentration. It seemed relevant to us to compare these results with those obtained for tsitsikammamine analogues which were the subject of a previous work (Figure 4).[9] Compounds **1** and **21** which are open structures have the same inhibition capacity against IDO, the nature of the aromatic substituent at the end of the chain and the presence of a hydroxyl group does not seem to have much influence on the activity. Compounds **3** and **4** are less active than their counterpart compounds in which the second five-membered cycle is not aromatic. This is in agreement with the previous observation which showed that the fully aromatic analogue of **22b** had an activity reduced by half. None of the aza-analogues evaluated in this work, except compound **19**, showed activity against IDO, **19** inhibiting the enzyme to a moderate level. In general, contrary to what one would have expected, given the activity of Roxyl-WL, the replacement of a pyrrole ring by a pyrrazole ring, did not lead to better inhibitors.

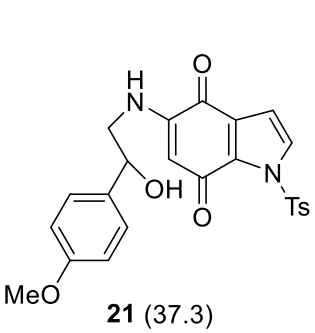

21 (37.3)

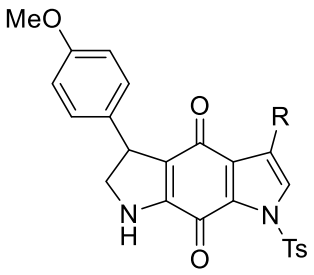

22a, R = H (54.2)
22b, R = H (40.2)
23a, R = $CH_2CH_2NH_2$ (40.2)

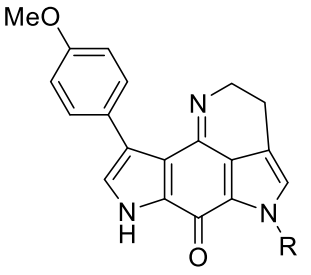

R = Ts, **24** (32)
R = H, **25b** (19.4)

Figure 4*: Tsitsikammamine analogues studied in a previous work and exhibiting the best inhibitory activities (the percentage obtained at 10 μM is indicated in brackets), a and b refer to iso1 and iso2.*

The best IDO1 inhibitors in this series and in this family so far, are compounds **5** and **6** which are also the only ones comprising an additional substituent in α-position of the nitrogen of the substituted pyrrole ring.

Three derivatives **1**, **5** and **19** are dual inhibitors, as they also show activity against TDO, the most active being compound **5** whereas none were active in the previous series.

Molecular docking

In order to understand the affinity observed within IDO1, we studied the binding mode of compounds by molecular docking[18] using Molegro Virtual Docker program.[19] Prior to modelling studies, a classification of know Protein Data Bank (PDB)[20] structures related to Uniprot P14902 domain[21] was done. The PDB structures were split and all chains structurally aligned against 2D0T[22] (chain A, formerly 2D0Ta) using UCSF Chimera/MatchMaker.[23,24] The resulting 52 chains were clustered using a combination of descriptors at protein or ligand levels, resulting in five groups. The 2DTOa (used for structural alignment) and 5EK2a[25] (used for docking as target) were included in the same group (5EK2a being the representative of a sub-cluster characterized by a binding cavity a little more opened). Two docking protocols were used: P1-GPU for screening and P2-OPT (full flexibility of binding site) for investigating the best compounds **5** and **6** (supplementary data for the overall in silico processes). The key interactions stabilizing the compounds within the IDO binding cleft are depicted in Figures 5 and 6 respectively (2D interactions diagrams are available in supplementary data).

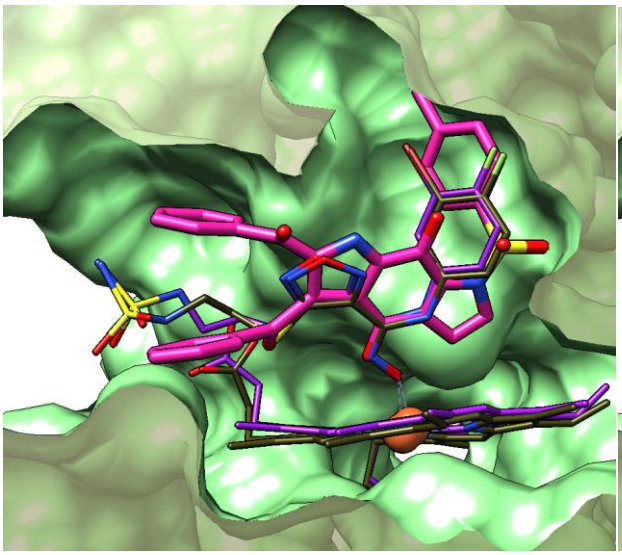

Figure 5: Best **5** docked pose (pink, big sticks) of **5** in 5EK2a binding site (light green, molecular surface) relatively to crystallographied ligands BBJ (purple, from 6E40, chain A) and HQS (kaki, from 6E41, chain A) after structural alignment.

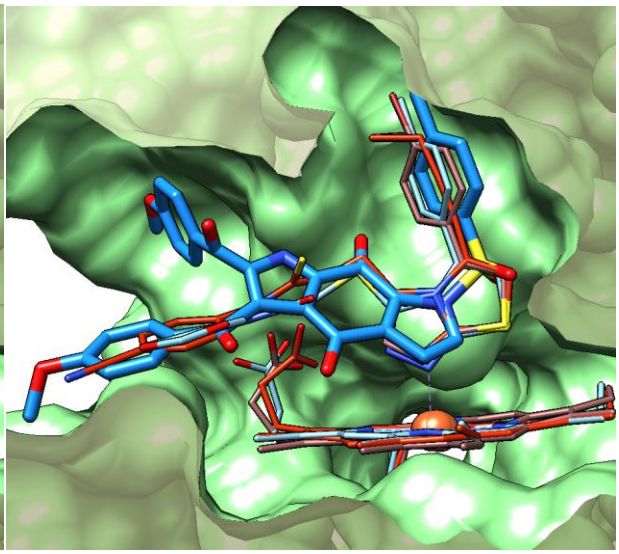

Figure 6: Best **6** docked pose (blue, big sticks) of **6** in 5EK2a binding site (light green, molecular surface) relatively to crystallographied ligands DO9 (red, from 6KOFa), PKJ (light blue, from 4PK5a) and DYC (brown, from 6KW7a) after structural alignment.

BBJ and HQS are found in PDB structures 6E40 and 6E41.[26] These two structures are classified in the same cluster 2D0Ta. The tosyl (Ts) group allows the classical L shaped form upper the heme's plane and shows interactions (hydrogen bonds) with SER167 and TYR126. The cycles (Ts and bispyrrololoquinonic frame) are found in the same plane as most of the IDO1 ligands complexed with heme whereas the phenyl groups share non unusual placement with compounds found in structures of IDO1 at entry of binding cavity (Figure 6 for an example). Interestingly, one of the two carbonyl groups of **5** is aligned with the hydroxylamine of BBJ and HQS.

The best pose of **6** is different from its counterpart **5**, but shares the overall T shaped form, allowed by the placement of Ts group inside the cavity and normal to the heme. The Ts group exhibits the same interaction (hydrogen bond) with SER167. Some similarities (shape, planes) are found with known ligands of IDO1, particularly D09, PKJ and DYC from 4PK5 (chain A), 6KOF (chain A) and 6KW7 (chain A) respectively.[27,28] These protein structures are classified in the same cluster than 5EK2a used for the docking studies. The pattern of interactions is different from the one of **5**, with more involvement of Pi (cycles, cations, sulfur) interactions. Interestingly, one of five-membered cycles of **6** is very well placed over the heme center, even if a nitrogen atom is not found in front of the Fe.

In conclusion, derivatives of marine pyrroloquinolines wakayin and tsitsikammamine have shown in a cell-based assay, interesting inhibitory activity on IDO1 and TDO, two enzymes involved in tumoral immune resistance. A molecular modeling study of compounds **5** and **6** in the IDO1active site gives insights to optimize these compounds. Particularly the impact of one of the two carbonyl groups of **5** close enough to Fe could be investigated to make electrostatic interactions as in the case of the hydroxylamine group of BBJ. In compound **6**, the replacement of a carbon by a nitrogen capable of dative bonding with Fe would be a first approach before further optimizing the compound to create a second interaction involving the carboxyl group of heme.

References

1- Brochez, L.; Chevolet, I.; Kruse, V. *Eur. J. Cancer*, **2017**, *76*, 167-182.

2- Ye, Z.; Yue, L.; Shi, J.; Shao, M.; Wu, T. *J. Cancer*, **2019**, *10*, 2771-2782.

3- Labadie, B. W.; Bao, R.; Luke, J. J. *Clin. Cancer Res.* **2019**, *25*, 1462-1471.

4- Carr, G., Chung, M. K. W.; Mauk, A. G.; Andersen R. J. *J. Med. Chem*. **2008**, *51*, 2634-2637.

5- Copp, B. R.; Ireland, C. M.; Barrows, L. R. *J. Org. Chem.* **1991**, *56*, 4596-4597.

6- Hooper, G. J.; Davies-Coleman, M. T.; Borges, K.; Coetze, P. S. *Tetrahedron Lett.* **1996**, *37*, 7135-7138

7- Rives, A.; Delaine, T.; Legentil, L.; Delfourne, E. *Tetrahedron Lett.* **2009**, *50*, 1128.

8- Rives, A.; Le Calvé, B.; Delaine, T.; Legentil, L. Kiss, R.; Delfourne, E. *Eur. J. Med. Chem.* **2010**, *45*, 343.

9- Dolusic, E.; Larrieu, P.; Meinguet, C.; Colette, D.; Rives, A.; Blanc, S.; Ferain, T.; Pilotte, L. ; Stroobant, V. ; Wouters, J. ; Van den Eynde, B.; Masereel, B. ; Delfourne, E.; Frédérick, R. *Bioorg. Med. Chem. Lett.* **2013**, *23*, 47-54.

10- Xu, G.; Wang, T.; Li, Y. ; Huang, Z. ; Wang, X. ; Zheng, J.; Yang, S.; Fan, Y.; Xiang, R. *J. Enz. Inhib. Med. Chem.* **2018**, *33*, 1089-1094.

11- Zhang L.; Cava, M. P.; Rogers, R. D.; Rogers, L. M. *Tetrahedron Lett*, **1998**, *39*, 7677

12- Farwaha, H. S.; Bucher, G.; Murphy, J. A. *Org. Biomol. Chem.* **2013**, *11*, 8073–8081

13- Chassaing, S.; Delfourne, E. *Magn. Res. Chem.* **2010**, *47*, 9.

14- Vanicat, A.; André-Barrès, C.; Delfourne, E. *Tetrahedron Letters* **2017**, *58*, 342-345.

15- Legentil, L.; Lesur, B.; Delfourne, E. *Bioorg. Med. Chem. Lett.* **2006**, *16*, 427.

16- Legentil, L.; Benel, L.; Bertrand, V.; Lesur, B.; Delfourne, E. *J. Med. Chem.* **2006**, *49*, 2979.

17- Luc Pilotte, L; Larrieu, P.; Stroobanta, V.; Colaua, D.; Dolušic, E.; Frédérick, R. ; De Plaena, E. ; Uyttenhovea, C. ; Wouters, J. ; Bernard Masereel, B. ; Van den Eynde, B. *PNAS* **2012**, *109*, 2497-2502.

18- Sousa, S. F.; Ribeiro, A. J. M.; Coimbra, J. T. S.; Neves, R. P. P.; Martins, S. A.; Moorthy, N. S. H. N.; Fernandes, P. A.; M.J. Ramos, P. A. *Curr. Med. Chem.* **2013**, 20: 2296-2314.

19- Thomsen, R.; Christensen, M. H. *J. Med. Chem.* **2006**, *49*, 3315-3321.

20- Berman, H. M.; Westbrook, J.; Feng, Z.; Gilliland, G.; Bhat, T. N.; H. Weissig, N.; Shindyalov, I. N.; Bourne, P. E. *Nucleic Acids Research* **2000**, *28*, 235-242.

21- The UniProt consortium. *Nucleic Acids Res.* **2019**, 47, D506-515.

22- Sugimoto, H.; Oda, S. I.; Otsuki, T.; Hino, T.; Yoshida, T.; Shiro, Y. *Proc Natl Acad Sci USA* **2006**, *103*, 2611-2616.

23- Pettersen, E. F.; Goddard, T. D.; Huang, C. C.; Couch, G. S.; Greenblatt, D. M.; E.C. Meng, Ferrin, T. E. *J. Comput. Chem.* **2004**, 25, 1605-1612.

24- Meng, E. C.; Pettersen, E. F; Couch, G. S.; Huang, C. C.; Ferrin, T. R. *BMC Bioinformatics* **2006**, *7*, 339-349.

25- Peng, Y. H.; Ueng, S. H.; Tseng, C. T.; Hung, M. S.; Song, J. S.; Wu, J. S.; Liao, F. Y.; Fan, Y. S.; Wu, M. H.; Hsiao, W. C.; Hsueh, C. C.; Lin, S. Y.; Cheng, C. Y.; Tu, C. H.; Lee, L. C.; Cheng, M. F.; Shia, K. S.; Shih, C.; Wu, S. Y.; Y.H. Peng, Y. H. *J. Med. Chem.* **2016**, *59*, 282-293.

26- Luo, S.; Xu, K.; Xiang, S.; Chen, J.; Chen, C.; Guo, C.; Tong, Y.; Tong, L. *Acta Crystallogr. F Struct. Biol. Commun.* **2018**, *74*, 717-724.

27- Tojo, S.; Kohno, T.; Tanaka, T.; Kamioka, S.; Ota, Y.; Ishii, T.; Kamimoto, K.; Asano, S.; Isobe, Y. *ACS Med. Chem. Lett.* **2014**, *5*, 1119-1123.

28- Peng, Y. H.; Liao, F. Y.; Tseng, C. T.; Kuppusamy, R.; Li, A. S.; Chen, C. H.; Fan, Y. S.; Wang, S. Y.; Wu, M. H.; Hsueh, C. C.; Chang, J. Y.; Lee, L. C.; Shih, C.; Shia, K. S.; Yeh, T. K.; Hung, M. S.; Kuo, C. C.; Song, J. S.; Wu, S. Y.; Ueng, S. H. *J. Med. Chem.* **2020**, *63*, 1642-1659.

Supplementary data

IDO1 and TDO inhibitory evaluation of analogues of the marine pyrroloiminoquinone alkaloids:wakayin and tsitsikammamines

Thomas Levy[a], Laura Marchand[a], Vincent Stroobant[b], Luc Pilotte[b], Benoît Van den Eynde[b], Frédéric Rodriguez[a] and Evelyne Delfourne[a,*]

Chemistry: ^{1}H and ^{13}C NMR spectra were performed on Bruker Avance 300 or Avance 500 (cryoprobe TCI $^{1}H\{^{13}C, ^{31}P\}$) spectrometers with the chemical shifts of the remaining protons of the deuterated solvents serving as internal standards. IR spectra were obtained on a Thermo Nicolet 6700 spectrophotometer. Mass spectra were recorded on a GCT premier waters mass spectrometer for CI and High resolution mass spectra (HRMS) were recorded on a UPLC Xevo G2 Q TOF Waters spectrometer for ESI. Reagents were purchased from commercial sources and used as received. Flash-chromatography was performed on silica gel (15-40 μM) by means of the solvent systems indicated below.

5-((2-(1H-indol-3-yl)ethyl)amino)-1-tosyl-1H-indole-4,7-dione (**1a**) and *6-((2-(1H-indol-3-yl)ethyl)amino)-1-tosyl-1H-indole-4,7-dione* (**2a**) and 5-((2-(1H-indol-3-yl)ethyl)amino)-1H-indole-4,7-dione (**1**) and 6-((2-(1H-indol-3-yl)ethyl)amino)-1-tosyl-1H-indole-4,7-dione (**2**)

To a solution of 1-tosyl-1H-indole-4,7-dione (480 mg, 1.59 mmol) in absolute ethanol (140 mL) was added portionwise tryptamine (1.3 g, 7.95 mmol) and the mixture was stirred at room temperature for 2h. After concentration over vacuum, the crude product was purified by flash-chromatography (CH_2Cl_2) to give the expected compounds: (CH_2Cl_2) to give the two expected compounds **1a** and **2a** and the elution solvent was changed (CH_2Cl_2/MeOH 99: 1 to give the second ones **1** and **2**:

1a: pink fuschia solid (59 mg, 8%), 166 °C. HRMS (DCI-CH_4) calcd for $C_{25}H_{22}N_3O_4S$ 460.1331, found 460.1331. ^{1}H NMR ($CDCl_3$): 2.45 (s, 3H); 3.12 (t, 2H, J = 6.9

* Corresponding author, Tel 33 561 55 62 93 ; Fax 33 561 55 60 11
E-mail : delfourn@chimie.ups-tlse.fr

Hz); 3.43 (q, 2H, J = 6.9 Hz); 5.26 (s, 1H) 5.84 (br t, 1H, J = 5.6 Hz); 6.67 (d, 1H, J = 3.3 Hz); 7.07 (d, 1H, J = 2.4Hz); 7.16 (td, 1H, J = 1Hz and 8 Hz); 7.25 (td, 1H, J = 1 Hz and 8 Hz); 7.36 (d, 2H, J = 8.2 Hz); 7.41 (d, 1H, J = 8.2 Hz); 7.59 (d, 1H, J = 7.8 Hz); 7.70 (d, 1H, J = 3.3 Hz); 8.04 (d, 2H, J = 8.2 Hz); 8.10 (br s, 1H). ^{13}C NMR ($CDCl_3$) 21.78, 24.05, 42.77, 97.49, 107.16, 111.40, 112.00, 118.43, 119.70, 122.16, 122.44, 126.83, 126.93, 127.71, 129.13 (2C), 129.46 (2C), 132.69, 134.27, 136.43, 145.85, 147.02, 175.08, 178.82. IR (ATR) 3357, 1678, 1593, 1371 cm^{-1}.

2a: pink fuschia solid (80 mg, 11%), mp 111 °C. HRMS (DCI-CH_4) calcd for $C_{25}H_{22}N_3O_4S$ 460.1331, found 460.1343. ^{1}H NMR (CDCl3): 2.53 (s, 3H, CH_3); 3.10 (t, 2H, J = 6.6 Hz); 3.43 (q, 2H, J = 6.7 Hz); 5.37 (s, 1H); 5.93 (t, 1H, J = 5.6 Hz); 6.74 (d, 1H, J = 3.1 Hz); 7.06, (d, 1H, J = 2.3 Hz); 7.15 (dq; 1 H, J = 1Hz and 7 Hz); 7.24 (dq, 1H, J = 1 Hz and 7Hz); 7.35 (d, 2H, J = 1Hz and 8.7 Hz); 7.41 (td, 1H, J = 1 Hz and 8.2 Hz); 7.58 (dd, 1H, J = 1 Hz and 7.9 Hz); 7.81 (d, 1H, J = 3.2 Hz); 7.99 (d, 2H, J = 8.4 Hz); 8.16 (br s, 1H). ^{13}C NMR ($CDCl_3$) 21.79, 24.13, 42.95, 96.64, 108.62, 111.41, 111.95, 118.46, 119.67, 122.20, 122.42, 126.91, 126.92, 128.87 (2C), 129.79 (2C), 131.27, 133.95, 134.53, 136.46, 146.17, 148.09, 170.12, 181.37. IR (ATR) 3308, 1653, 1632, 1375 cm^{-1}.

1: pink fuschia solid (224 mg, 46%), mp 228 °C. HRMS (DCI-CH_4) calcd for $C_{18}H_{16}N_3O_2$ 306.1243, found 306.1247. ^{1}H NMR (DMSO-d_6) 3.01 (t, 2H, J = 7.4 Hz); 3.40 (q, 2H, J = 6.9 Hz); 5.21 (s,1H), 6.41 (d, 1H, J = 2.5 Hz); 7.00 (td, 1H, J = 1.1 Hz and 8 Hz); 7.09 (td, 1H, J = 1Hz and 8 Hz); 7.15 (t, 1H, J = 5.9 Hz); 7.25 (t, 1H, J = 2.5 Hz); 7.26 (s, 1H, J = 1.8 Hz); 7.36 (d, 1H, J = 8Hz); 7.56 (d, 1H, J = 8Hz); 10.88 (br s, 1H, NH); 12.62 (br s, 1H, NH). ^{13}C NMR (DMSO-d_6) 23.73, 43.38, 107.40, 111.65, 111.90, 118.67, 118.81 (2C), 121.22, 123.50, 124.11, 127.57, 134.80, 136.72, 150.03, 177.13, 178.37. IR (ATR) 3420, 3288, 1673, 1603, 1392cm^{-1}.

2: pink fuschia solid (107 mg, 22%), mp 209 °C. HRMS (DCI-CH_4) calcd for $C_{18}H_{16}N_3O_2$ 306.1243, found 306.1230. ^{1}H NMR (DMSO-d_6): 3.01 (t, 2H, J = 7.4 Hz); 3.42 (q, 2H, J = 6.9 Hz); 5.20 (s, 1H) 6.48 (d, 1H, J = 2.5 Hz); 7.00 (m, 2H); 7.08 (td, 1H, J = 1Hz and 8 Hz); 7.25 (d, 1H, J = 2.5 Hz); 7.32 (t, 1H, J = 5.9 Hz); 7.35 (d, 1H, J = 8Hz); 7.57 (d, 1H, J = 8Hz); 10.87 (br s, 1H, NH); 12.41 (br s, 1H, NH). ^{13}C NMR (DMSO-d_6) 23.76, 43.34, 96.31, 107.92, 111.71, 111.89, 118.67, 118.80, 121.46, 123.46, 127.59, 128.42, 128.60,129.20, 136.72, 148.89, 172.30, 182.20. IR (ATR) 3388, 1654, 1623, 1600, 1397 cm^{-1}.

5-((2-(1H-indol-3-yl)ethyl)(methyl)amino)-1-tosyl-1H-indole-4,7-dione (**1b**) and *6-((2-(1H-indol-3-yl)ethyl)(methyl)amino)-1-tosyl-1H-indole-4,7-dione* (**2b**)

A solution of methyl tryptamine (1.09 g, 6.3 mmol) in absolute ethanol (15 mL) was added dropwise to a solution of indoledione **21** (0.38 g, 1.25 mmol) in absolute ethanol (16 mL). After 2h stirring at room temperature, the mixture was concentrated over vacuum and the crude product was purified by flash-chromatography (CH_2Cl_2/MeOH 99.5: 0.5) to give the expected compounds:

1b: pink fuschia solid (180 mg, 12%), mp 175 °C. HRMS (DCI-CH_4) calcd for $C_{26}H_{23}N_3O_4S$ 474.1488, found 474.1483. ^{1}H NMR ($CDCl_3$) 2.45 (s, 3H), 2.95 (s, 3H), 3.10 (t, 2H, J = 7.2 Hz), 3.97 (t, 2H, J = 7.2 Hz), 5.34 (s, 1H), 6.55 (d, 1H, J = 3.3 Hz), 7.00 (d, 1H, J = 2.2 Hz), 7.16 (m, 2H), 7.36 (d, 2H, J = 8.1 Hz), 7.63 (d, 1H, J = 3.3 Hz), 8.05 (d, 2H, J= 8.1 Hz). ^{13}C NMR ($CDCl_3$) 21.78, 24.38, 41.11, 56.10, 104.49, 107.69, 111.18, 112.45, 118.79, 119.66, 122.28, 122.65, 127.02, 127.42, 128.80, 129.10 (2C), 129.44, 131.09 (2C), 134.54, 136.31, 145.75, 151.28, 174.22, 184.42. IR (ATR) 3366, 1674, 1624, 1369 cm^{-1}.

2b: pink fuschia solid (710 mg, 48%), mp 175 °C. HRMS (DCI-CH_4) calcd for $C_{26}H_{23}N_3O_4S$ 474.1488, found 474.1491. ^{1}H NMR ($CDCl_3$) 2.43 (s, 3H), 2.98 (s, 3H), 3.11 (t, 2H, J = 7.2 Hz), 3.92 (t, 2H, J = 7.2 Hz), 5.38 (s, 1H), 6.66 (d, 1H, J = 3.3 Hz), 7.08 (d, 1H, J = 2.2 Hz), 7.22 (m, 2H), 7.39 (d, 2H, J = 8.1 Hz), 7.64 (br.s, 1H), 7.75 (d, 1H, J = 3.3 Hz), 8.13 (d, 2H, J= 8.1 Hz). ^{13}C NMR ($CDCl_3$) 21.76, 24.28, 41.01, 55.67, 103.82, 107.56, 111.18, 112.57, 118.98, 119.72, 122.27, 122.59, 127.19, 127.33, 128.98, (2C), 129.65 (2C), 130.22, 132.20, 134.49, 136.24, 145.90, 152.80, 175.08, 183.67. IR (ATR) 3365, 1670, 1618, 1370 cm^{-1}.

3-(1H-indol-3-yl)-1-methyl-5-tosyl-2,3-dihydropyrrolo[2,3-f]indole-4,8(1H,5H)-dione (**3**)

To a solution of compound **2a** (140 mg, 0.3 mmol) in CH_2Cl_2 (9 mL), was added DDQ (140 mg, 0.6 mmol). The mixture was stirred for 2h at room temperature. After concentration over vacuum, the crude product was purified by flash-chromatography (CH_2Cl_2/MeOH 99.5: 0.5) to give the expected product as a violin solid (40 mg, 28%), mp > 260 °C. HRMS (DCI-CH_4) calcd for $C_{26}H_{20}N_3O_4S$ 470.1175, found 470.1173. ^{1}H NMR ($CDCl_3$) 2.43 (s, 3H), 4.10 (s, 3H), 6.78 (d, 1H, J = 3.3 Hz), 7.17-7.27 (m, 3H), 7.33 (d, 2H, J = 8.4 Hz), 7.48 (d, 1H, J = 8.2 Hz), 7.72 (d, 1H, J = 7.8 Hz), 7.76 (d, 1H, J = 3.3 Hz), 8.04 (d, 2H, J = 8.4 Hz), 8.25 (d, 1H, J= 3.0 Hz), 8.35 (br. s, 1H). ^{13}C NMR ($CDCl_3$) 21.74, 36.94, 107.43, 107.68, 111.52, 119.64, 120.21, 120.31, 122.12, 126.22, 126.78, 128.95, 128.98 (2C), 129.16, 129.49 (2C),

129.87, 131.49, 132.54, 134.60, 136.01, 145.58, 171.84, 174.06. IR (ATR) 3369, 1646, 1629, 1376 cm^{-1}

3-(1H-indol-3-yl)-1-methyl-7-tosylpyrrolo[3,2-f]indole-4,8(1H,7H)-dione (**4**)

Same procedure as for compound **3** involving compound **2b** (200 mg, 0.4 mmol), CH_2Cl_2 (12 mL) and DDQ (200 mg, 0.9 mmol). Purification by flash-chromatography (CH_2Cl_2/MeOH 99.5: 0.5) led to the expected product as a violin solid (150 mg, 75%), mp > 260 °C. HRMS (DCI-CH_4) calcd for $C_{26}H_{20}N_3O_4S$ 470.1175, found 470.1157. ^1H NMR ($CDCl_3$) 2.47 (s, 3H), 4.07 (s, 3H), 6.81 (d, 1H, J = 3.2 Hz), 7.24 (m, 2H), 7.21-7.27 (m, 3H), 7.38 (d, 2H, J = 8.5 Hz), 7.46 (d, 1H, J = 7.3 Hz), 7.77 (d, 1H, J = 3.2 Hz), 8.07 (d, 2H, J = 8.5 Hz), 8.35 (br. s, 1H), 8.39 (d, 1H, J= 3.2 Hz). ^{13}C NMR ($CDCl_3$) 21.78, 37.28, 107.74, 108.34, 111.59, 119.57, 119.80, 120.30, 122.17, 122.21, 126.13, 126.70, 128.82, 128.92 (2C), 129.29, 129.59 (2C), 130.49, 130.61, 133.90, 134.53, 136.09, 145.79, 167.13, 178.84. IR (ATR) 3306, 1652, 1631, 1374 cm^{-1}.

Determination of IDO1 and TDO activities: the assay was performed in 96-well flat bottom plates seeded with 2 10^5 cells in a final volume of 200 µL. To determine TDO or IDO activity, the cells were incubated overnight at 37 °C in IMDM supplemented with 2% FBS (Invitrogen). The plates were then centrifuged 10 min at 300 g, and 150 µL of the supernatant were collected. The supernatant was analyzed by HPLC to measure the concentration of residual tryptophan and produced kynurenine, based on the retention time and the UV absorption (280 nm for tryptophan, 360 nm for kynurenine). For the HPLC analysis, 55 µL of supernatant were mixed with 55 µL of 6% (wt/vol) trichloroacetic acid to precipitate the proteins. After centrifugation, the supernatant (100 µL) was collected and injected onto an Onyx Monolithic C18 column (Phenomenex). The inhibition of tryptophan degradation and kynurenine production was expressed as a percentage of the values obtained in the absence of inhibitor. A dose/response assay was then performed at four concentrations. For each compound, the cell viability, expressed in percentage, was evaluated at the end of the incubation period.

Structural classification, molecular visualization and molecular docking

Molecular graphics were performed with the UCSF Chimera package. Chimera is developed by the Ressource for Biocomputing, Visualization, and Informatics at the University of California, San Francisco (supported by the NIGMS P41-GM103311).

The protein structures used in this paper were downloaded from the RCSB Protein Database and were structurally aligned with structure 2DT0 (chain A, formerly cited as 2DT0a) set as reference and using UCSF Chimera/Matchmaker program. The protein structures, were prepared (structure checks, rotamers, hydrogenation, splitting of chains) using Biovia (www.3dsbiovia.com) Discovery Studio Visualizer 2016 (DSV) and UCSF Chimera.
The new compounds were sketched using ChemAxon Marvin 16, (www.chemaxon.com).
All ligands were checked (hybridization, hydrogenation, some geometry optimizations, 3D sketching) and merged in SDF libraries using DSV.

The structural classification is based on combination of descriptors (at ligand and protein levels) such as position, orthogonal projection, decomposition for ligands, presence for cofactor, aperture level for protein, interaction networks. All the chains of 48 IDO1 liganded (heme or ligands) structures corresponding to Uniprot domain P14902 were spitted, individually aligned and the similar chains were reduced to one representative structure. Finally the 52 chains studied were classified in five clusters, and a representative structure was chose for each cluster. The first cluster [A] is characteristic of an opened binding cavity and was mainly subdivided in [A] opened) and [A1] (more opened). The [A] cluster was represented by the reference chain 2DT0a and included 2D0Ua, 4U72a, 4U74a, 6E40a, 6E42c, 6E41a, E41b, 5XE1a, 5W8Na chains. The [A1] cluster was represented by 5EK2a used for docking studies and included 4PK5a, 4PK5b, 4PK6a, 4PK6b, 5EK4a, 5EK3a, 5EK2a, 5ETWa, 6PU7b, 6KW7a, 6KOFa, 6KPSa, 6O3Ia, 6V52a, 6WJY chains.

Molecular modeling studies were carried with Molegro Virtual Docker 6 software (www.clcbio.com) using the A chain of structure 5EK2a as target.
A search space volume of 15 Å radius centered in the binding pocket around ligand 5PJ (from 5EK2a) was used. The ligands were set flexible during the docking, and two different docking protocols (P1-GPU and P2-OPT) were used.
The protocol P1-GPU is based on rigid docking at protein level and a GPU (Nvidia Tesla CUDA hardware, www.nvidia.com) screening algorithm. Docking process used the MolDock function (Moldock [grid] with a resolution of 0.3 Å) for scoring and CUDA optimizer (MVD, 6000 iteration steps, other parameters let as default, no water molecule was taken in account during calculations. The protocol returns 100 independent runs. Post-docking, all the poses were re-ranked using MolDock and Rerank scoring systems.

The protocol P2-OPT is based on flexible docking at protein level (softened potentials during docking phase) and Moldock optimizer was used as searching algorithm. According to structural study, 20 residues were defined as flexible during the docking: ALA260, ALA264, ARG231, CYS129, GLN266, ILE354, LEU154, LYS238, MET295, PHE163, PHE164, PHE226, SER167, SER235, SER263, TYR126, TYR233, VAL125 and VAL130. Docking process used 3000 iteration steps, (convergence was reached for all ligands) other parameters let as default. The protocol returns 20 independent runs. A final minimization (per run) was parameterized using 2000 steps for lateral chains and protein backbone; other parameters were let with default values. A displaceable water molecule was taken in account in the calculations. MolDock and Rerank scores were calculated post-docking and post-minimization.

The two protocols used a pharmacophoric model (template) with a grid resolution of 0.3 Å and strength of 500. The definition of template was based on aligned protein structures in the same reference space. The conformations of co-crystallized IDO1 complexes making coordinate bonding involving the nitrogen of ligand and Fe of heme, showed clearly that it was possible to set a minimal template based on the mean position of nitrogen. Four similarity groups (using spheres of 1.8 Å radiuses) and one atom per group were defined as ring, negative charge, hydrogen acceptor, steric hindrance.

The clustering parameters (RMSD threshold 1.7 Å, other parameters let as default) were the same for P1-GPU and P2-OPT protocols.

The protocol P1-GPU was used on all ligands and worked well with fragment-like molecules; the crystallographic reproduction of 5PJ conformation of 5EK2a was reached with a RMSD of 0.62 Å. As protocol P2 gave similar orientation of tosyl groups in the binding site, the best compounds were investigated using P2-OPT protocol and full site flexibility. As controls, the PKJ (from 4PK5a and ROX ligands were docked in 5EK2a in order to check the reproduction of crystallography (RMSD of 1.47 Å) and docking results (same conformation and orientation). We noticed also that 5EK2a and 4PK5a are included in the same protein structural cluster (open++ class).

DSV generated 2D interaction diagram of **5** best pose (best Rerank) using protocol OPT.

Two groups of hydrogen bonds are found, the first for oxygen of Ts group (two interactions), the other implying one of the carbonyl group and Heme (one interaction and potent metal donor/acceptor).

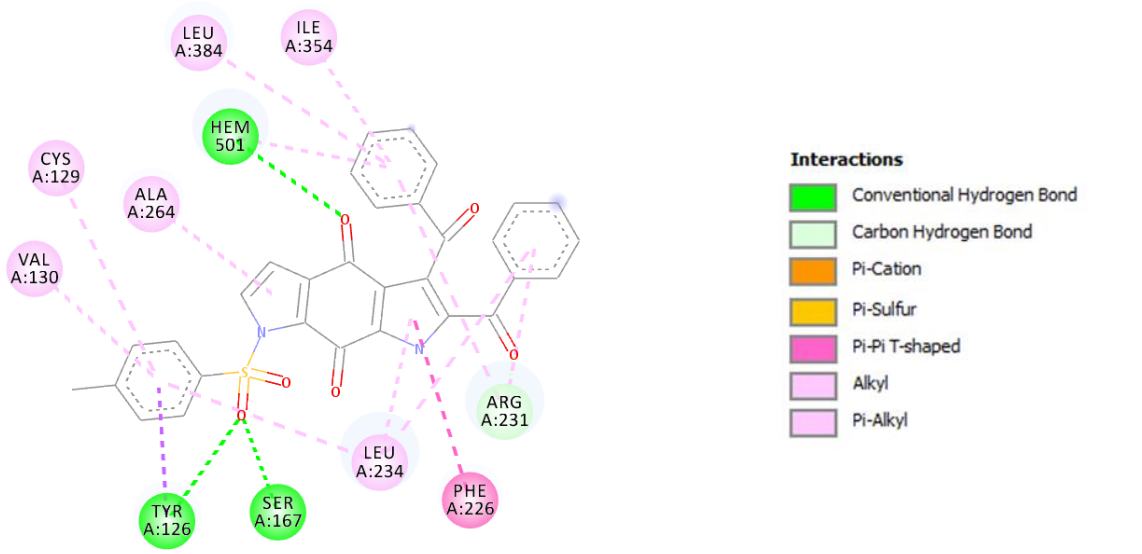

DSV generated 2D interaction diagram of **6** best pose (best Rerank) using protocol OPT.

Three hydrogen bonds are found for this compound with additional Pi-sulfur (CYS129) and Pi-Cation (ARG231) interactions. The corresponding pose of **6** is close to the Heme center than in the case of the counterpart **5**.